LETTERS

Slip zone and energetics of a large earthquake from the Taiwan Chelungpu-fault Drilling Project

Kuo-Fong, Ma[1], Hidemi Tanaka[2], Sheng-Rong Song[3], Chien-Ying Wang[1], Jih-Hao Hung[1], Yi-Ben Tsai[1], Jim Mori[4], Yen-Fang Song[5], Eh-Chao Yeh[6], Wonn Soh[6], Hiroki Sone[7], Li-Wei Kuo[3] & Hung-Yu Wu[1]

Determining the seismic fracture energy during an earthquake and understanding the associated creation and development of a fault zone requires a combination of both seismological and geological field data[1]. The actual thickness of the zone that slips during the rupture of a large earthquake is not known and is a key seismological parameter in understanding energy dissipation, rupture processes and seismic efficiency. The 1999 magnitude-7.7 earthquake in Chi-Chi, Taiwan, produced large slip (8 to 10 metres) at or near the surface[2], which is accessible to borehole drilling and provides a rare opportunity to sample a fault that had large slip in a recent earthquake. Here we present the retrieved cores from the Taiwan Chelungpu-fault Drilling Project and identify the main slip zone associated with the Chi-Chi earthquake. The surface fracture energy estimated from grain sizes in the gouge zone of the fault sample was directly compared to the seismic fracture energy determined from near-field seismic data[3,4]. From the comparison, the contribution of gouge surface energy to the earthquake breakdown work is quantified to be 6 per cent.

The North–South-trending Chelungpu fault is a major 90-km structure that dips shallowly to the east (30°), and principally slips within, and parallel to, bedding of the Pliocene Chinshui shale[5]. Taiwan Chelungpu-fault Drilling Project (TCDP) drilled two vertical holes 40 m apart (hole A to a depth of 2 km, and hole B to a depth of 1.3 km), and a side-track from hole B (hole C) at the depth of 950 m to 1,200 m about 2 km east of the surface rupture, near the town of DaKeng (Fig. 1a). The subsurface location of the Chinshui shale was known from high-resolution seismic reflection profiles[6,7] at a depth of about 1,000 m under the DaKeng site. The spatial slip distribution for the earthquake was well constrained from close strong motion stations and Global Positioning System (GPS) data[3,4] and shows a slip of 8.3 m on the fault near the drill site. The drilling carried out continuous coring for depths of 500–2,000 m for hole A, 950–1,300 m for hole B and 950–1,200 m for hole C, respectively. Geophysical well logs were carried out in hole A to collect seismic velocities, densities and digital images.

From the hole-A core, the Chelungpu fault zone is seen within the Chinsui shale as a damaged zone at depths of about 1,105 to 1,115 m, consisting of fault breccia and fault gouge (Fig. 1b). The degree of fracturing increases from the top to the bottom of the zone. Near the bottom of the broad zone of deformation, a 12-cm-thick primary slip zone (PSZ) can be identified based on the presence of ultra-fine-grained fault gouge and increased fracture density at depths of 1,111.23 to 1,111.35 m. A corresponding feature was also found in the hole-B core at depths of 1,136.50 to 1,136.62 m, confirming the fault dip of 30° E. The geophysical logging measurements of low seismic velocities and low electrical resistivity around the depth of 1,111 m also confirm that this is the main fault zone.

The PSZ seen in the core from hole C after splitting and polishing (Fig. 1c), shows several layers of slip zones associated with several repeating earthquakes. The individual slip zone has a thickness of about 2–3 cm with a 5-mm ultrafine grain zone in the bottom as indicated in the PSZ schematic (Fig. 1c). Among the slip zones, the least deformed region, which has the fewest number of cross-cutting cracks, is the 2-cm zone at the bottom of the PSZ, suggesting that this narrow band might be the major slip zone (MSZ) that corresponds to the Chi-Chi earthquake. Other estimates of the thickness for the slip zone from nearby sites are 50–300 μm observed at the surface near the DaKeng drill site[8], and 7 mm from a fault core at a depth of 330 m in shallow drilling before TCDP[9]. These determinations of slip zone thicknesses are all from layers located near the bottom of the fracture zone. The variation of thickness of the slip zone at different depths might correspond to differences in normal stress[10–12].

We also analysed the grain size distribution of the slip zone[13,14] using transmission electron microscope (TEM), scanning electron microscope (SEM) and optical microscope measurements, to estimate the surface fracture energy associated with the gouge formation. The distribution of particle size is shown in Fig. 2a, which follows a power-law distribution with a slope of about 2.3 (refs 15 and 16; see Supplementary Information). Grain sizes of 50 nm–100 mm (Fig. 2b, Supplementary Fig. 1a–c) were observed for the 2-cm MSZ (Supplementary Table 1). We consider grain sizes larger than 50 nm for the surface fracture energy calculation. The images with grain sizes of less than 50 nm show rounded shapes, suggesting that those small grains might be the result of precipitation rather than fracturing (Fig. 2b). Assuming spherical grains and a ratio of surface area to volume for spheres of 3/radius (ref. 13), we obtained the total particle surface area for the 2-cm slip zone S_{MSZ} of 6.46×10^5 m^2 per metre squared area. The mineral composition from X-ray diffraction for semiquantitative analysis shows that the MSZ was composed of about 70% of quartz, 5% of feldspar, and 25% of clay minerals (Supplementary Fig. 2). This gives a specific fracture energy G_c of about 1 J m^{-2} (refs 17–19). Using a correction for grain roughness λ of 6.6 (ref. 20), and the specific fracture energy, we obtain the surface fracture energy G_{MSZ} of the 2-cm MSZ by:

$$G_{MSZ} = S_{MSZ}\lambda G_c \quad (1)$$

From equation (1), we obtain a value of 4.3 MJ m^{-2} for the surface fracture energy. This is interpreted as the minimum amount of energy that is necessary to produce the MSZ in one earthquake.

[1]Department of Earth Sciences, National Central University, Chung-Li 32054, Taiwan. [2]Department of Earth and Planetary Sciences, University of Tokyo, Tokyo 113-0033, Japan. [3]Department of Geosciences, National Taiwan University, Taipei 10617, Taiwan. [4]Disaster Prevention Research Institute, Kyoto University, Kyoto 611-0011, Japan. [5]National Synchrotron Radiation Research Center, Hsinchu 30076, Taiwan. [6]Kochi Institute for Core Sample Research, Agency for Marine-Earth Science and Technology, Kochi 783-8502, Japan. [7]Department of Geology and Mineraology, Kyoto University, Kyoto 606-8501, Japan.

Any additional contribution to the estimated surface fracture energy from considering a much wider, but less deformed, damage zone is thought to be less than 10% of the above value[13].

Formation of the slip zone is associated with the seismic fracture energy, which is consumed as the earthquake rupture propagates. The creation of small grains is a contribution, but may not be the total equivalent to the seismic fracture energy. To estimate the seismic fracture energy from the observed earthquake waves, we used a three-dimensional finite difference code based on the traction-at-split nodes method to calculate the stress time history on the earthquake fault plane[21], with the temporal–spatial slip distribution inverted from strong motion data[4] as a constraint. The seismic fracture energy density on the fault is determined by retrieving the dynamic traction evolution during the slip history.

The breakdown work[22] W_b, which is the excess work over some minimum level achieved during slip, is the energy spent to allow the rupture to advance. It can be obtained from the slip history of shear traction on the fault, by calculating the integral of the traction versus slip, from zero slip to the point that the traction drops to a minimum:

$$W_b = \int_0^{T_b} (\boldsymbol{\tau}(t) - \boldsymbol{\tau}_{\min}) \cdot \mathbf{v}(t) \mathrm{d}t \qquad (2)$$

where $\mathbf{v}(t)$ is the slip velocity, $\boldsymbol{\tau}(t)$ is the shear traction, and T_b is the time at which minimum traction $\boldsymbol{\tau}_{\min}$ is reached. A grid size of 0.95 km and a time interval of 0.054 s were used for the calculation. Figure 3 shows the shear traction change as a function of slip and time for the particular portion of the fault beneath the borehole site. The shaded area in Fig. 3 corresponds to the integral in equation (2), and gives a value for the breakdown work W_b of 11.6 MJ m^{-2}. This value is comparable to that for other nearby subfaults, and the results of other studies[23]. This breakdown work can be considered as an equivalent to the seismic fracture energy density[22] G_s. The breakdown work derived from the equation (2) is composed of the surface fracture energy for formation of the slip zone, and other dissipative losses during faulting[22]. Here, we assume that the fault core thickness, fault geometry, clast grain size and distribution retrieved from TCDP do not significantly change over the subfault area of the seismic inversion.

The geological studies[5,8] show that the total displacement accommodated by the Chelungpu–Chinshui detachment, where the TCDP drilled through, is 0.3 km. Considering the 12-cm primary slip zone identified from the retrieved core, the ratio (T/D) of the slip thickness ($T = 12$ cm) to the total displacement ($D = 300$ m) is 4×10^{-4}. For the 8.3-m slip of the Chi-Chi earthquake, the slip thickness for a single earthquake is 3.3 mm. This means that the number of events in the 2-cm MSZ is between 6 and 7 if we assume similar displacements of repeating earthquakes in the major slip zone. For the 4.3 MJ m^{-2} of the surface fracture energy from the 2-cm MSZ, the fracture surface energy associated to a single earthquake on average would be about 0.65 MJ m^{-2}. Given that the breakdown work is 11.6 MJ m^{-2}, this value shows that the process of grain formation represents about 6% of the earthquake breakdown work. We consider this estimate to be the maximum for the assumption that there is no fracture energy occurred during sliding[13]. The remaining part of the breakdown work will mostly be heat, which might be associated with other dynamic processes, such as fault thermopressurization[24–26], or fault lubrication[27,28].

The radiation efficiency η_R is the ratio of the radiated energy E_R to the energy available for mechanical processes. It was defined[29] as $\eta_R = \frac{E_R}{E_R + E_G}$, where E_G is the product of fault area and seismic fracture energy density. Here, we consider the seismic fracture energy in the equation to be the surface energy used to pulverize the rock for

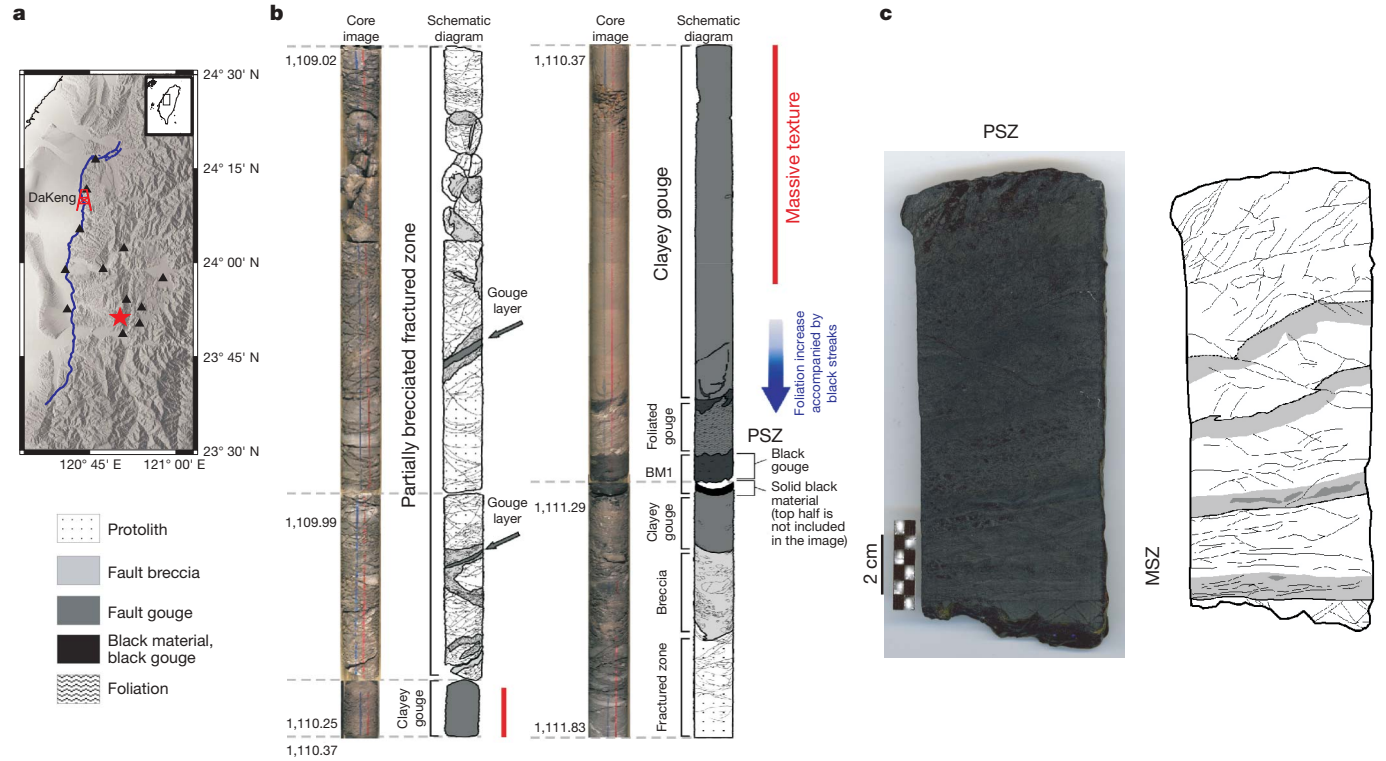

Figure 1 | Location, core images and polished primary slip zone. **a**, The location of the drill site at the town DaKeng and the ruptured Chelungpu fault (bold blue line). The black triangles show the distribution of the strong motion stations close to the fault. The epicentre is shown by a red asterisk. **b**, The core image and schematic diagram from the depths of 1,109.02 m to 1,111.83 m of hole A with descriptive comments. A 12-cm primary slip zone was observed at the depth of 1,111.23–1,111.35 m. **c**, An enlarged photo of the splitting and polishing slab of the 12-cm principal slip zone (PSZ) with its schematic. The thicker lines in the schematic indicate the possible slip zones associated with several repeating earthquakes. The 5-mm ultrafine grain zone in the bottom of each layer is shown in grey. The bottom layer with the less-deformed slip zone is the major slip zone (MSZ) related to the 1999 Chi-Chi earthquake.

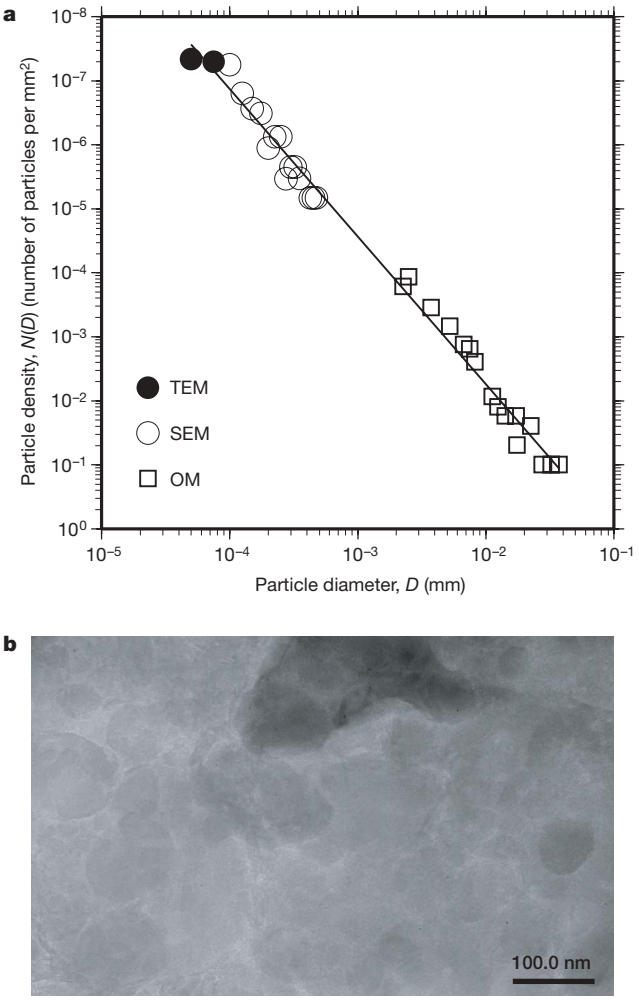

Figure 2 | Particle size in the major slip zone. a, Distribution of the particle size, $N(D)$ as a function of particle diameter (D) in millimetres. The $N(D)$ is the number of grains per mm^2 for a class of grain size. The measurements are imaged from TEM (solid circles), SEM (circles), and optical (square). The regression of the particle size distribution follows the power law $N(D)=aD^{-b}$, where a is 0.0045 and b is 2.3. **b**, TEM image; scale, 100 nm.

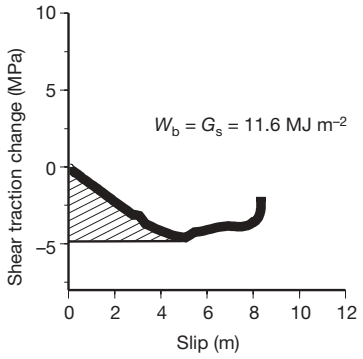

Figure 3 | The slip-weakening curve for the fault block corresponds to the borehole site. The shaded area gives an estimate for W_b, equivalent to G_s, of about 11.6 MJ m^{-2}.

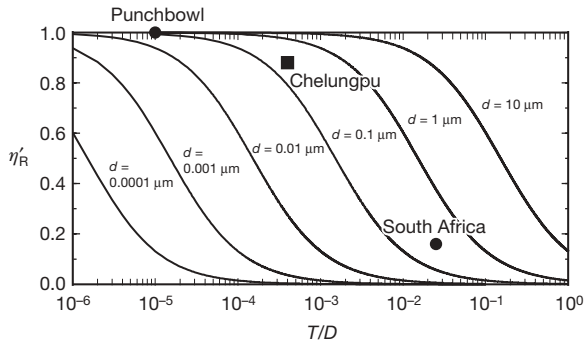

Figure 4 | The ratio of radiated energy to the summation of the radiated and surface energy as a function of the ratio of fault thickness (*T*) to total fault displacement (*D*). Curves show the values for various grain sizes. The values for the Punchbowl fault, South African mines (solid circles) and the Chelungpu fault (squares) are shown. The Chelungpu fault has intermediate values between the Punchbowl fault (1.0) and data from the South African mines (0.16).

formation of the fault gouge. Assuming that the ratio of the seismic energy to seismic moment is constant, η_R can be modified to the quantity[1]:

$$\eta'_R = \frac{1}{1+\frac{6\lambda}{\mu C_R}\left(\frac{T}{D}\right)\left(\frac{G_c}{\hat{d}}\right)} \quad (3)$$

where $C_R = E_R/M_o$, and M_o is the seismic moment. The value of C_R is 2×10^{-5}, using values of E_R and M_o for the Chi-Chi earthquake derived from seismic data[4,30]. The representative grain size $\hat{d}$ has a value of 186 nm from $\hat{d} = 6T/S_{MSZ}$, which has an amount of surface fracture energy equivalent to that of the power-law size-distribution in the MSZ. If the surface energy is the major contribution to the fracture energy, η'_R will have a similar value to η_R. For a rigidity $\mu = 30$ GPa, we obtain a value of η'_R of 0.88 for the Chlungpu fault (Fig. 4).

The gouge zone of the Chelungpu fault for the Chi-Chi earthquake was formed as a result of about 6% of the breakdown work. The calculated value for η'_R is intermediate between that of the well-developed Punchbowl fault in California[13] ($\eta'_R \approx 1.0$) and those of the earthquakes in a South African mine that are ($\eta'_R \approx 0.16$) associated with making new fractures[18]. The physical differences in the fault zones may depend on the maturity and style of faulting[13] and reflect the differences in the mechanical energy absorbed during large events. When large earthquakes occur on mature faults, there is less fracturing, so the proportional amount of dissipative energy is smaller, compared to the more brittle behaviour of young faults.

Received 28 February; accepted 13 September 2006.

1. Kanamori, H. The diversity of the physics of earthquakes. *Proc. Jpn. Acad.* **80**, 297–316 (2004).
2. Ma, K-F. *et al.* The Chi-Chi, Taiwan earthquake: large surface displacements on an inland thrust fault. *Eos* **80**, 605 (1999).
3. Ma, K-F. *et al.* Spatial and temporal distribution of slip for the 1999 Chi-Chi, Taiwan earthquake. *Bull. Seismol. Soc. Am.* **91**, 1069–1087 (2001).
4. Ji, C. *et al.* Slip history dynamic implications of the 1999 Chi-Chi, Taiwan, earthquake. *J. Geophys. Res.* **108**, 2412, doi:10.1029/2002JB001764 (2003).
5. Yue, L. F., Suppe, J. & Hung, J-H. Structure geology of a classic thrust belt earthquake: the 1999 Chi-Chi earthquake Taiwan (Mw=7.6). *J. Struct. Geol.* **27**, 2058–2083 (2005).
6. Wang, C-Y. Detection of a recent earthquake fault by the shallow reflection seismic method. *Geophysics* **67**, 1465–1473 (2002).
7. Wang, C-Y., Li, C-L. & Yen, H-Y. Mapping the northern portion of the Chelungpu fault, Taiwan by shallow reflection seismics. *Geophys. Res. Lett.* **29**, doi:10.1029/2001GL014496 (2002).
8. Heermance, R., Shipton, Z. K. & Evans, J. P. Fault structure control on fault slip and ground motion during the 1999 rupture of the Chelungpu fault, Taiwan. *Seismol. Soc. Am. Bull.* **93**, 1034–1050 (2003).
9. Tanaka, H. *et al.* Initial science report of shallow drilling penetrating into the Chelungpu fault zone, Taiwan. *Terr. Atmos. Ocean. Sci.* **113**, 227–251 (2002).
10. Sibson, R. H. Thickness of the seismic slip zone. *Bull. Seismol. Soc. Am.* **93**, 1169–1178 (2003).
11. Tanaka, H. *et al.* Whole fault zone architecture and its relation to thin slip layer activated by 1995 Kobe earthquake detected at 1140 m depth in the drilled core penetrating the Nojima fault. *J. Geophys. Res.* (submitted).
12. Gratier, J-P., Favreau, P. & Renard, F. Modeling fluid transfer along California faults when integrating pressure solution crack sealing and compaction process. *J. Geophys. Res.* **108**, doi:10.1029/2001JB000380 (2003).

13. Chester, J. S., Chester, F. M. & Kronenberg, A. K. Fracture surface energy of the Punchbowl Fault, San Andreas system. *Nature* **437,** 133–136 (2005).
14. Sammis, C., King, G. & Biegel, R. The kinematics of gouge deformation. *Pure Appl. Geophys.* **125,** 777–812 (1987).
15. Otsuki, K., Monzawa, N. & Nagase, T. Fluidization and melting of fault gouge during seismic slip: Identification in the Nojima fault zone and implications for focal earthquake mechanisms. *J. Geophys. Res.* **108,** B4 2192, doi:10.1029/2001JB001711 (2003).
16. Kadono, T. *et al.* Surface roughness of alumina fragments caused by hypervelocity impact. *Planet. Space Sci.* **54,** 212–215 (2006).
17. Scholz, C. H. in *The Mechanics of Earthquakes and Faulting* 158–167 (Cambridge Univ. Press, Cambridge, UK, 2002).
18. Lawn, B. *Fracture of Brittle Solids* 2nd edn 1–378 (Cambridge Univ. Press, New York, 1993).
19. McGarr, A., Spottiswoode, S. M. & Gay, N. C. Observations relevant to seismic driving stress, stress drop, and efficiency. *J. Geophys. Res.* **84,** 2251–2261 (1979).
20. Wilson, B., Dewers, T., Reches, Z. & Brune, J. Particle size and energetics of gouge from earthquake rupture zones. *Nature* **434,** 749–752 (2005).
21. Andrews, D. J. Test of two methods for faulting in finite-difference calculations. *Bull. Seismol. Soc. Am.* **89,** 4931–4937 (1999).
22. Tinti, E., Spudich, P. & Cocco, M. Earthquake fracture energy inferred from kinematic rupture models on extended faults. *J. Geophys. Res.* 110, B12303 doi:10.1029/2005JB003644 (2005).
23. Zhang, W. B. *et al.* Heterogeneous distribution of the dynamic source parameters of the 1999 Chi-Chi, Taiwan, earthquake. *J. Geophys. Res.* **108,** doi:10.1029/2002JB001889 (2003).
24. Abercrombie, R. E. & Rice, J. R. Can observation of earthquake scaling constrain slip weakening? *Geophys. J. Int.* **162,** 406–424 (2005).
25. Wibberley, C. A. J. & Shimamoto, T. Earthquake slip weakening and asperities explained by thermal pressurization. *Nature* **436,** 689–692 (2005).
26. Tanaka, H. *et al.* Frictional heat from faulting of the 1999 Chi-Chi, Taiwan earthquake. *Geophys. Res. Lett.* **33,** doi:10.1029/2006GL026673 (2006).
27. Brodsky, E. & Kanamori, H. Elastohydrodynamic lubrication of faults. *J. Geophys. Res.* **106,** 16357–16373 (2001).
28. Ma, K-F. *et al.* Evidence for fault lubrication during the 1999 Chi-Chi, Taiwan, earthquake (Mw7.6). *Geophys. Res. Lett.* 30, 1244 doi:10.1029/2002GL015380 (2003).
29. Husseini, M. I. & Randall, M. J. Rupture velocity and radiation efficiency. *Seismol. Soc. Am. Bull.* **660,** 1173–1187 (1976).
30. Venkataraman, A. & Kanamori, H. Effect of directivity on estimates of radiated seismic energy. *J. Geophys. Res.* **109,** doi:10.1029/2003JB002548 (2004).

Supplementary Information is linked to the online version of the paper at www.nature.com/nature.

Acknowledgements We thank the working group of TCDP, including the drilling company FangYu and WonDa, the on-site assistants and more than 60 participating students from NCU and NTU, S. T. Huang at CPC for core storage and splitting, Y.-M. Chen of the NSRRC for taking TEM and TXM images, and K. S. Liang of the NSRRC. We also thank M. Zoback, S. Hickman, W. Ellsworth and H. Ito for discussion before and during drilling. We also thank H. Kanamori and E. Brodsky for discussions and a review of an early version of this paper. This project was supported by the NSC, Taiwan, and partially supported by the ICDP.

Author Contributions K.-F.M., paper writing and project planning. H.T., core observation, data analysis and project planning. S.-R.S., petrographic and XRD analysis and project planning. C.-Y.W., J.-H.H., Y.-B.T., W.S., project planning. J.M., paper preparation. Y.-F.S., TEM and TXM taken at NSRRC and data analysis. E.-C.Y. and H.S., on-site geologists during coring. L.-W.K. and H.-Y.W., on-site assistants.

Author Information Reprints and permissions information is available at www.nature.com/reprints. The authors declare no competing financial interests. Correspondence and requests for materials should be addressed to K.-F.M. (fong@earth.ncu.edu.tw).